ISSN 1753-3562

June 2012 Volume 53 Number 3

Physics and Chemistry of Glasses

European Journal of Glass Science and Technology Part B

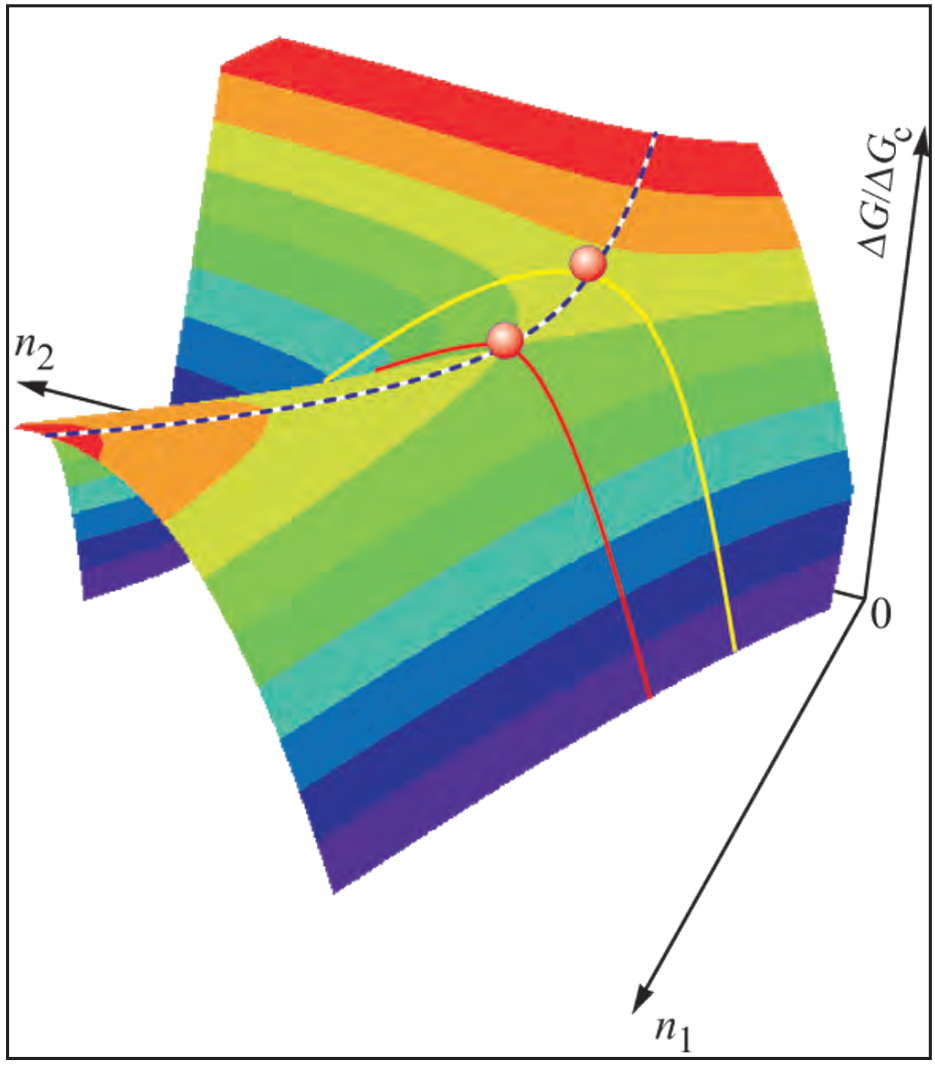

Volume 53 Number 3 June 2012

Physics and Chemistry of Glasses

European Journal of Glass Science and Technology B

CONTENTS

Cover: A detail taken from Figure 1 of the paper: Dependence of crystallization processes of glass-forming melts on melt history: a theoretical approach to a quantitative treatment by Jürn W. P. Schmelzer & Christoph Schick (*Phys. Chem. Glasses: Eur. J. Glass Sci. Technol. B*, June 2012, **53** (3), 99–106)

The European Journal of Glass Science and Technology is a publishing partnership between the Deutsche Glastechnische Gesellschaft and the Society of Glass Technology. Manuscript submissions can be made through Editorial Manager, see the inside back cover for more details.

Society of Glass Technology
9 Churchill Way
Chapeltown
Sheffield S35 2PY, UK
Tel +44(0)114 263 4455
Fax +44(0)8718754085
Email info@sgt.org
Web http://www.sgt.org

The Society of Glass Technology is a registered charity no. 237438.

Advertising
Requests for display rates, space orders or editorial can be obtained from the above address.

Physics and Chemistry of Glasses: European Journal of Glass Science and Technology, Part B
ISSN 1753-3562 (Print)
ISSN 1750-6689 (Online)

The journal is published six times a year at the beginning of alternate months from February.

Electronic journals: peer reviewed papers can be viewed by subscribers through Ingenta Select
http://www.ingentaconnect.com

Phys. Chem. Glasses: Eur. J. Glass Sci. Technol. B, June 2012, **53** (3), 121–127

SpectraFit: a new program to simulate and fit distributed ^{10}B powder patterns – application to symmetric trigonal borons

*Victor Khristenko, Kevin Tholen, Nathan Barnes, Evan Troendle, David Crist, Mario Affatigato, Steve Feller**

Physics Department, Coe College Cedar Rapids, IA 52402, USA

Diane Holland, Thomas F. Kemp & Mark E. Smith

Physics Department, University of Warwick, UK CV4 7AL, UK

Manuscript received 3 November 2011
Revised version received 22 December 2011
Accepted 2 March 2012

We have developed a new program in C++ to simulate ^{10}B NMR powder patterns. The program takes into account the quadrupolar interaction of ^{10}B (I=3) and it allows for the use of a Gaussian distribution of the quadrupolar interaction parameters to fit solid amorphous and crystalline materials. A key aspect of this program is that it has been automated to find the best-fit parameters of the quadrupole coupling constant (C_Q) and the asymmetry parameter (η) as well as the widths (σ_{CQ} and σ_η) of their distributions. Initially, this program has been extensively used, with the aid of the earlier and non-automatic QuadFit developed by Tom Kemp at the University of Warwick (UK), to find the best fit parameters of ^{10}B NMR spectra in amorphous B_2O_3 prepared at different cooling rates as well as polycrystalline lithium orthoborate, Li_3BO_3. The technique is sensitive enough to clearly see differences in the three-coordinated boron quadrupole parameters.

I. Introduction

The intermediate range order (IRO) in glass, at the level up to several angstroms or so, is currently of great interest. Nuclear magnetic resonance (NMR) in certain circumstances may be suited to the study of the IRO. Normally, we examine the short range order (SRO) with NMR since it uses the nucleus to probe its local and perhaps nearest neighbor bonding environments. However, modern NMR techniques such as dynamic angle spinning (DAS) or double rotation (DOR), or the examination of certain nuclei with especially strong interactions are sometimes able to reach out a bit further and probe the IRO in terms of superstructural borate groups for example.

^{10}B NMR is sensitive to this level of order within the glass since it has a very strong quadrupole interaction, with coupling constants (C_Q) that exceed 5 MHz for the three-coordinate borons. It also has a spin of 3 which produces six transitions which provides exquisite detail to exploit. The resulting experimental powder patterns are also extremely sensitive to the asymmetry parameter, η, as well as to distributions of C_Q and η. The standard deviations of the respective distributions are denoted σ_{CQ} and σ_η. The result is an ability to probe further into the glass structure, even beyond the SRO.

Over the past few years we have begun to systematically prepare borate glasses and crystals, enriched in ^{10}B at levels that exceed 95 atomic%, of differing superstructural groupings, to determine the above four quadrupole parameters that characterize short range borate structures in intermediate range structures. However, until now, we have not had the means to obtain the true best fit parameters.

We report on fitting ^{10}B NMR powder patterns using a new automated fitting procedure that we have named *SpectraFit*. This program is capable of determining these best four fit parameters for a given site within borate glasses and crystals. This approach allows us to determine the four quadrupole parameters *individually* to a high precision. Thus, we have the chance to observe borons in differing environments, even within different superstructual groups, by systematically changing boron environments in different crystals and glasses.

In this paper we used the new technique, with its added precision, to specifically examine polycrystalline lithium orthoborate and vitreous boron oxide prepared using three cooling rates spanning a range of 10^8 K/s. Each of these materials has a symmetric SRO consisting of a boron triangle with either all bridging oxygens (vitreous B_2O_3) or nonbridging oxygens (crystalline $Li_3B_3O_3$).

II. Procedures

Experimental and simulations

1. Sample preparation

Glassy boron oxide was prepared three ways using enriched ^{10}B (greater than 95 atomic%) boric acid.

*Corresponding author. Email sfeller@coe.edu
Original version presented at VII Int. Conf. on Borate Glasses, Crystals and Melts, Dalhousie University, Halifax, Nova Scotia, Canada, 21–25 August 2011

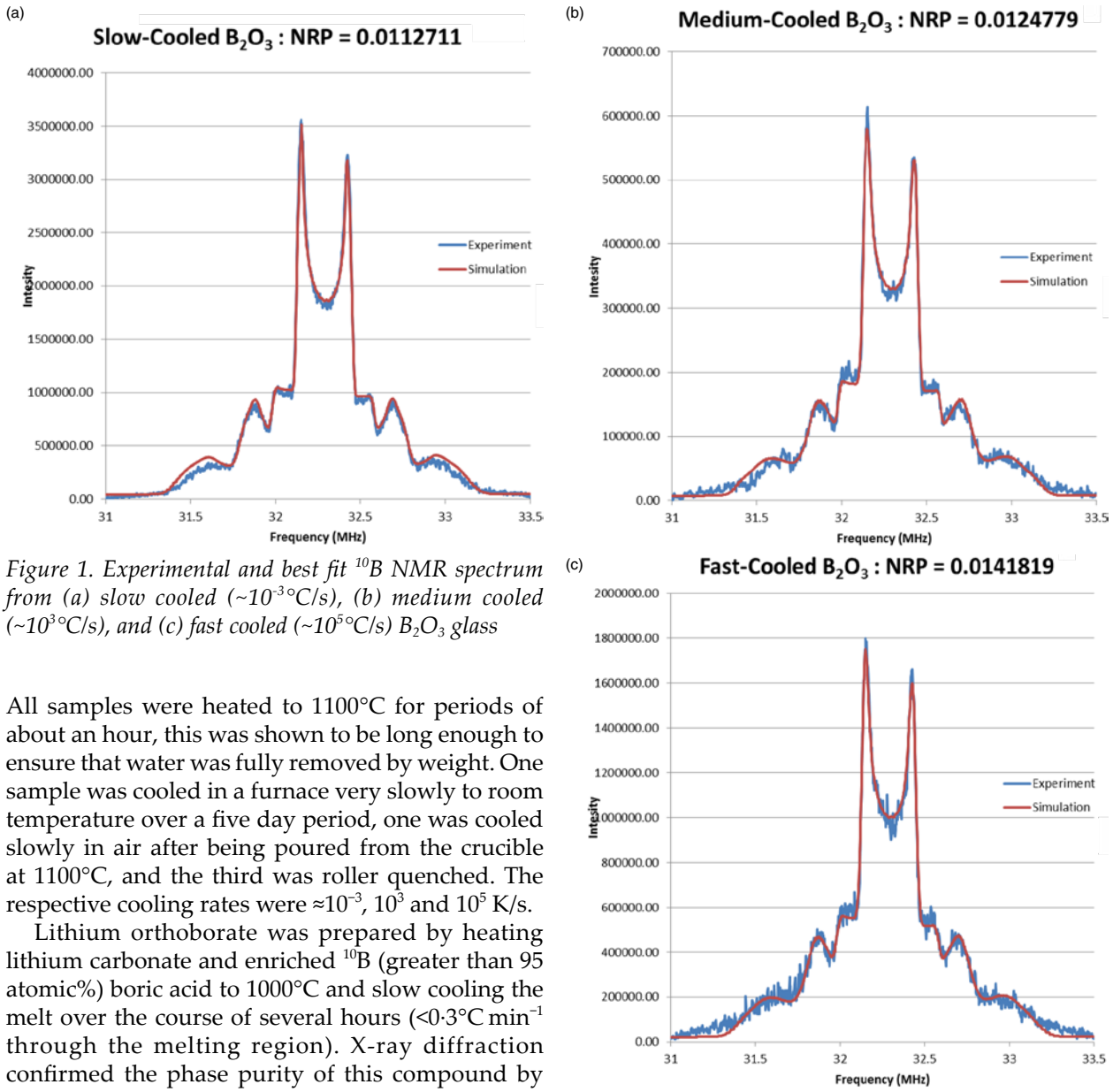

Figure 1. Experimental and best fit ^{10}B NMR spectrum from (a) slow cooled (~10^{-3}°C/s), (b) medium cooled (~10^{3}°C/s), and (c) fast cooled (~10^{5}°C/s) B_2O_3 glass

All samples were heated to 1100°C for periods of about an hour, this was shown to be long enough to ensure that water was fully removed by weight. One sample was cooled in a furnace very slowly to room temperature over a five day period, one was cooled slowly in air after being poured from the crucible at 1100°C, and the third was roller quenched. The respective cooling rates were ≈10^{-3}, 10^{3} and 10^{5} K/s.

Lithium orthoborate was prepared by heating lithium carbonate and enriched ^{10}B (greater than 95 atomic%) boric acid to 1000°C and slow cooling the melt over the course of several hours (<0·3°C min^{-1} through the melting region). X-ray diffraction confirmed the phase purity of this compound by comparison with the pattern calculated from the single crystal study of Stewner.[1] Furthermore, Raman spectra were obtained from the sample that confirmed the presence of the crystalline phase when compared with the data of Kamitsos *et al.*[2]

2. NMR

Standard static pulse-echo ($\pi/2\rightarrow\pi$) experiments were performed at 7·0 T at an operating frequency of 31·49 MHz with the following conditions: τ=3 ms and $\tau/2$=1·5 ms; 10–30 s pulse delay; 1 MHz spectrum width at each frequency. A novel aspect of the present work was the acquisition of spectra at several different magnetic fields through the use of a field-step unit. This was necessary because of the extreme width of the powder pattern. Typically a frequency range of 1·44 MHz was covered in 57·6 kHz steps, with 1500 to 2500 acquisitions taken at each frequency to give an acceptable signal-to-noise ratio. The final experimental powder pattern is the summation of the spectra obtained at each magnetic field. It was found that a significant number of steps (on the order of 25) were needed to avoid artifacts from the step size appearing in the spectrum.

3A. Simulating ^{10}B powder patterns:

The powder patterns were calculated from an original automated fitting program that used the third order perturbation theory developed by Jellison, Feller & Bray[3] and the calculational ideas developed by Kemp,[4] including an Alderman Grant interpolation.[5] Quadrupolar perturbed NMR frequencies were thus calculated, using six transitions weighted properly in terms of the quantum mechanical probabilities.[3] This resulted in an NMR powder pattern. The effects of the distribution of sites in a glass were achieved by assuming a Gaussian distribution for

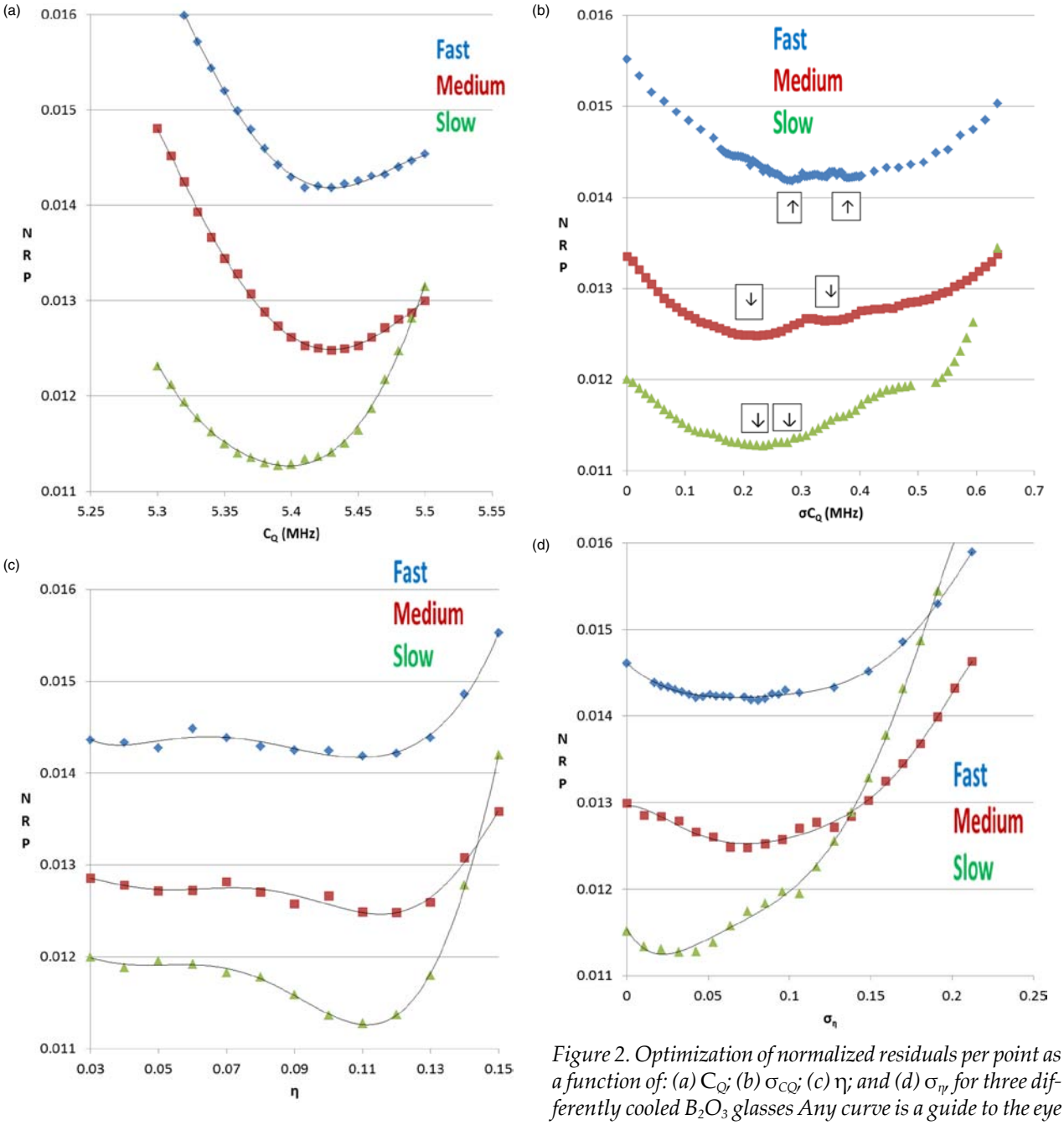

Figure 2. Optimization of normalized residuals per point as a function of: (a) C_Q; (b) σ_{CQ}; (c) η; and (d) σ_η, for three differently cooled B_2O_3 glasses Any curve is a guide to the eye

values of C_Q and η, whose standard deviations are σ_η, and σ_{CQ}, and summing the spectra simulated by the Gaussian function with up to 81 individual spectra to create a distributed spectrum.[6] The distributions were sampled out to +/− two standard deviations from the mean.

3B. SpectraFit fitting procedures

The distributed powder patterns were then calculated and compared to the experimental spectrum by the use of the *normalized residuals per point (NRP)*. The NRPs were minimized by searching systematically in the four-parameter space (C_Q, η, σ_η, and σ_{CQ}). This was done until plots of the NRP were made against optimized values for each of these four parameters. Minima in these plots represented best fit parameters from which the powder patterns were calculated. In some cases two minima were determined and these, we believe, represent two boron environments as will be discussed below.

III. Results

A. Vitreous B_2O_3

Experimental and best-fit simulated powder patterns were overlaid for the three differently cooled samples of ^{10}B enriched glassy boron oxide and these are shown in Figures 1(a, b and c). Figures 2(a)–(d) as well as Table 1 depict the results from the

Table 1. Quadrupole parameters from variously cooled boron oxide glasses (v-B_2O_3) and crystalline lithium orthoborate (c-Li_3BO_3)

Sample (B Site)	*Cooling rate (K/s)*	C_Q *(MHz)*	σ_{CQ} *(MHz)*	η	σ_η	*NRP*
v-B_2O_3 ring	10^5	5·43	0·382	0·11	0·042	0·0142125
v-B_2O_3 non-ring	10^5	5·43	0·285	0·11	0·081	0·0141819
v-B_2O_3 ring	10^3	5·44	0·340	0·11	0·053	0·0126468
v-B_2O_3 non-ring	10^3	5·43	0·223	0·12	0·074	0·0124779
v-B_2O_3 ring	10^{-3}	5·39	0·265	0·11	0·021	0·0113059
v-B_2O_3 non-ring	10^{-3}	5·39	0·234	0·11	0·032	0·0112711
c-Li_3BO_3		5·55	0·159	0·05	0·011	0·0152082

minimization of the NRP for each of the quadrupole parameters: C_Q, σ_{CQ}, η, and σ_η. We see in Figure 2(b) the plots of the quadrupole distribution width, σ_{CQ}, evidence for two boron sites. The resulting distribution width in η was used to distinguish the two boron sites, ring and non-ring borons. We assume the ring boron has a smaller σ_η than the non-ring boron since the asymmetry parameter is especially sensitive to deviations from axial symmetry as it is a measure of planar deviations of the electric field gradient in the principal axis system. Thus, we presume the rings are composed of rigid and planar borate triangles with less variation in this respect than the non-ring borons, Ref. 9 gives the mean ring internal B–O–B angle of 120·0± 0·7° with a small standard deviation of 3·2±0·4. For the external B(ring)–O–B(non-ring) the values are 135·1° and 6·7±0·4.

We note that σ_{CQ} is greater in the ring whereas η is the same or slightly smaller in the ring. Also, the smaller value of η in the ring for the medium cooled case is consistent with the site identification since this implies a more cylindrically symmetric site.

B. Polycrystalline Li_3BO_3

Experimental and simulated powder patterns were overlaid for polycrystalline Li_3BO_3 as shown in Figure 3. Figures 4(a)–(d) as well as Table 1 depict the results from the minimization of the NRP for each of the quadrupole parameters: C_Q, η, σ_η, and σ_{CQ}.

IV. Discussion

A. Boron oxide glass

Examination of Figures 2(a)–(d) indicates several interesting features. Figure 2(a) shows the NRP versus C_Q for the three boron oxide samples. The slow cooled sample displays a slightly lower C_Q than the two faster cooled samples, with a difference of only about 0·7%. Figure 2(b) for NRP versus σ_{CQ} shows the interesting presence of multiple minima as discussed above. Also present is the clear trend of σ_{CQ} decreasing in the region of the minima in NRP as we proceed from fast to slow cooled boron oxide glass. Further, Figures 2(b and d) indicate that the NRP trend versus distributions widths σ_{CQ} and σ_η become

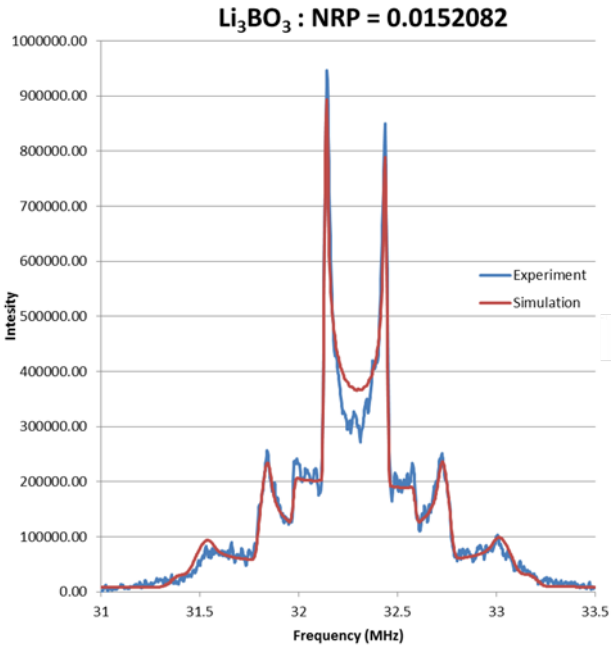

Figure 3. Experimental and best fit ^{10}B NMR spectrum from crystalline lithium orthoborate

more sharply defined as the cooling rate is lowered, this is especially true of the slow cooled sample in σ_η. Corroborating this result is the trend seen for η in Figure 2(c). While η hardly changes, the minimum in the NRP becomes much more clearly defined. All of these trends indicate more ordering taking place in the glass as the cooling rate is lowered by a factor of 10^8.

Numerous authors, using several techniques, have described the structure of boron oxide glass as being a composite of boroxol ring (B_R) and non-ring (B_{NR}) boron atoms with a ratio of approximately 3 or 4 to 1.[7] As indicated above on this basis we attributed the site with the lower asymmetry parameter distributions to the ring boron atoms and the site with the larger distributions to the non-ring boron atoms.

The literature contains several results that we can compare our data and simulations to. In 1978 Jellison, Panek & Bray[8] were able to observe two of the six ^{10}B NMR transitions from plate quenched (medium cooled) B_2O_3. Using the third order perturbation theory of Jellison, Feller & Bray[3] and by fitting an aspect of the resulting derivative powder pattern that was sensitive to distributions in the asymmetry parameter they determined a single site fit with:

$$C_Q = 5{\cdot}51 \text{ MHz} \quad (1a)$$

$$\sigma_{CQ} = 0{\cdot}21 \text{ MHz} \quad (1b)$$

$$\eta = 0{\cdot}12 \quad (1c)$$

$$\sigma_\eta = 0{\cdot}05 \quad (1d)$$

Taking the average of our two sites for our medium

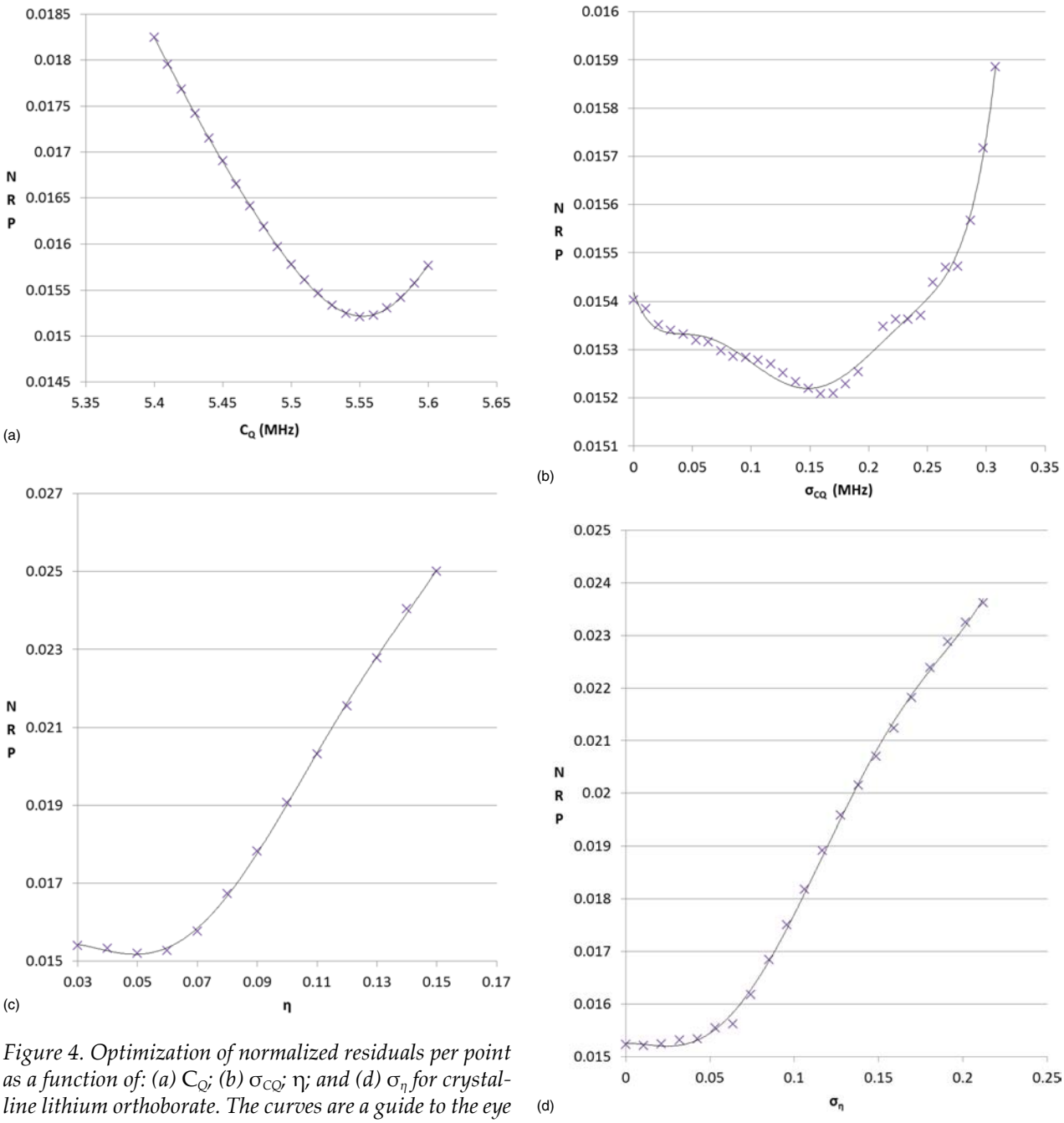

Figure 4. Optimization of normalized residuals per point as a function of: (a) C_Q; (b) σ_{CQ}; η; and (d) σ_η for crystalline lithium orthoborate. The curves are a guide to the eye

cooled sample gives:

C_Q=5·44 MHz (2a)

σ_{CQ}=0·28 MHz (2b)

η=0·12 (2c)

σ_η=0·064 (2d)

The agreement is quite reasonable.

The quadrupole interaction parameter, P_Q, is defined by

$$P_Q=C_Q(1+\eta^2/3)^{0.5} \quad (3)$$

and was recently measured by double rotation (DOR) ^{11}B NMR experiments by Dupree & Holland.[9] They reported values for P_Q and σP_Q in their paper using a medium cooled sample and found:

$P_Q(B_R)$=2·67 MHz (4a)

$P_Q(B_{NR})$=2·61 MHz (4b)

$\sigma P_Q(B_R)$=0·08 MHz (4c)

$\sigma P_Q(B_{NR})$=0·12 MHz (4d)

Using the ratios of the quadrupole moments of ^{10}B and ^{11}B we can find $C_Q(^{11}B)$ from $C_Q(^{10}B)$:

$$C_Q(^{11}B)=(Q^{B11}/Q^{B10})*C_Q(^{10}B)=(1/2{\cdot}084)*C_Q(^{10}B) \quad (5)$$

Using Table 1 and Equations (1) and (4) we deduced the following values for the ^{11}B P_Q and σP_Q from our ^{10}B NMR results for our medium cooled sample:

$P_Q(B_R)$ (from ^{10}B)=2·62 MHz (6a)

$P_Q(B_{NR})$ (from ^{10}B)=2·61 MHz (6b)

$\sigma P_Q(B_R)$ (from ^{10}B)=0·17 MHz (6c)

$\sigma P_Q(B_{NR})$ (from ^{10}B)=0·12 MHz (6d)

The agreement is seen to be good for the frequencies and fairly close for the distribution values. The assignment of the two boron sites from ^{10}B is consistent with the ^{11}B analysis in that the two techniques both observed the higher C_Q for the ring borons.

Finally, Bray *et al* performed nuclear quadrupole resonance measurements (NQR) on boron oxide glass and found two peaks.[10] The quadrupole frequencies, ν_{BR} and ν_{BNR} as well as $\sigma\nu_{BR}$ and $\sigma\nu_{BNR}$ for the ^{11}B NQR responses in the ring and non-ring borons were found to be:

ν_{BR}=1·357 MHz (7a)

ν_{BNR}=1·305 MHz (7b)

and

$\sigma\nu_{BR}$=0·00837 MHz (7c)

$\sigma\nu_{BNR}$=0·00972 MHz (7d)

The quadrupole resonance frequency is ½P_Q or

$$\nu_Q = \frac{C_Q}{2}\left(\frac{1+\eta^2}{3}\right)^{0.5} \quad (8)$$

Use of our ^{10}B results yields the following comparisons to the NQR data:

ν_{BR} (from ^{10}B)=1·308 MHz (9a)

ν_{BNR} (from ^{10}B)=1·306 MHz (9b)

and from our distributions in the quadrupole parameters

$\sigma\nu_{BR}$ (from ^{10}B)=0·085 MHz (9c)

$\sigma\nu_{BNR}$ (from ^{10}B)=0·059 MHz (9d)

The frequencies agree reasonably well whereas the distributions do not. The distributions are lower in the NQR data when compared with the ^{10}B NMR results.

B. Polycrystalline Li_3BO_3

On the whole it is still a very reasonable fit although overall the NRP for polycrystalline Li_3BO_3 is somewhat worse compared to those of boron oxide (0·01521 versus 0·01264). We are confident in the purity of the sample as it was checked both by x-ray diffraction and Raman spectroscopy, as discussed above. In particular, the central feature shows a poorer fit compared to the rest of the spectrum. One likely explanation is the possible preferred orientation of the crystalline powder in the NMR probe. Also, the crystal reasonably exhibits smaller distributions in the quadrupole parameters leading to inherently sharper features indicative of smaller distribution widths. A single minimum was found for the four quadrupole parameters as given in Table 1. This is consistent with the published crystal structure of Stewner[1] which indicates only one crystallographically distinct B site. The value of η=0·05 makes sense for a short range unit consisting of isolated $(BO_3)^{3-}$ triangles whose oxygens are all nonbridging. Indeed, η is smaller for this case compared to v-B_2O_3 where the boron triangles in the rings are bonded to both ring and non-ring borons and all borons have a larger variation in bond angles. In Figures 4(a)–(d) the minima are sharper than in the case of boron oxide presumably because of the less variability in bond angles and lengths in the crystal. The sharpness of the NRP minimum for η and σ_η near 0·05 and 0·01, respectively, is especially evident in Figures 4(c) and (d) and is indicative of the highly symmetric $(BO_3)^{3-}$ isolated borate triangles with nonbridging oxygens.

A few reports of quadrupolar parameters from orthoborate anions in lithium borate glasses, have been given in the literature. In 1978 Yun reported[11] the C_Q and η for the orthoborate anion from ^{11}B NMR in ($(BO_3)^{3-}$+3Li^+) to be (average):

$C_Q(^{11}B)$=2·66 MHz (10a)

η=0·08 (10b)

The corresponding present values from ^{10}B NMR and converted to ^{11}B values using Equation (5) are:

C_Q (^{11}B converted from ^{10}B)=2·66 MHz (11a)

η=0·05 (11b)

The agreement is good.

In 1982 Feller, Dell & Bray[12] were able to observe two of the six ^{10}B NMR transitions from plate quenched (medium cooled) lithium borate glasses of high lithia content. They determined for the orthoborate anion fit parameters of:

C_Q=5·75 MHz (12a)

σ_{CQ}=0·22 MHz (12b)

η=0·00 (12c)

σ_η=0·05 (12d)

The comparison values for crystalline Li_3BO_3 are

found in Table 1:

C_Q=5·55 MHz (13a)

σ_{CQ}=0·159 MHz (13b)

η=0·05 (13c)

σ_η=0·011 (13d)

C_Q and η are each a little different in the crystal compared with the glass parameters.

The distribution parameters, σ_{CQ} and σ_η, are each lower in the crystal than found in the glass; this is a sensible result.

V. Conclusions

We have demonstrated that an automatic fitting routine was effectively used in the fitting of ^{10}B NMR spectra from borate glasses and crystals. The fitting is able to examine distributions of the quadrupole parameters. This allowed us to find two boron sites in each of the glassy boron oxide samples as well a single boron site in polycrystalline lithium orthoborate. The two sites in v-B_2O_3 are attributed to ring and non-ring borons. Importantly, we saw increased ordering in the slow cooled boron oxide glass compared with the two faster cooled samples through a close examination of its quadrupole parameters. In particular the distribution widths narrowed as the cooling rate changed by a factor of 10^8.

VI. Acknowledgements.

The National Science Foundation is acknowledged for support of this work through grant NSF-DMR-0904615.

VII. References

1. Stewner, F. *Acta Cryst*., 1971, **B27**, 904.
2. Chryssikos, G. D., Kamitsos, E. I., Patsis, A. P., Bitsis, M. S. & Karakassides, M. A. *J. Non-Cryst. Solids*, 1990, **196**, 42.
3. Jellison, Jr, G. E., Feller, S. A. & Bray, P. J. *J. Mag. Res*., 1977, **27**, 121–132.
4. Kemp, T. F. & Smith, M. E. *Solid State Nucl. Magn. Resonance*, 2009,**35** (4), 243–252.
5. Alderman, D. W., Solum, M. S. & Grant, D. M. *J. Chem. Phys*., 1986, **84** (7), 3717.
6. In some instances, when η was near zero and the distribution would have required non-physical (-η) values, fewer than 81 spectra were used.
7. See summary in Wright, A. C. *Phys. Chem. Glasses: European J. Glass Science Technol. B*, 2010, **51** (1), 1–39.
8. Jellison Jr. G. E., Panek, L. W., Bray, P. J. & Rouse Jr. G. B. *J. Chem. Phys*., 1977, **66**, 802.
9. Hung, I., Howes, A. P., Parkinson, B. G, Anupold, T., Samoson, A., Brown, S. P., Harrison, P. F., Holland, D. & Dupree, R. *J. Solid State Chem*., 2009, **182**, 2402–2408.
10. Bray, P. J., Emerson, J. F., Lee, D. H., Feller, S., Bain, D. L. & Feil, D. A. *J. Non-Cryst. Solids*, 1991, **129**, 240–248.
11. Yun, Y. H. PhD Thesis, Brown University, 1978.
12. Feller, S., Dell, W. J. & Bray, P. J. *J. Non-Cryst. Solids*, 1982, **51**, 21–30.